Adiabatic Theory of Resonant Particle Dynamics with Frequency-Chirping Chorus Waves in Inhomogeneous Magnetic Fields

Jiangshan Zheng,[1] Ge Wang,[2] and Bo Li[1]

[1] *School of Physics, Beihang University, Beijing, 100191, China*
[2] *Center for Plasma Theory and Computation, Madison, Wisconsin 53706, USA*

(Dated: April 13, 2024)

We present the adiabatic regime for the particles interacting with the frequency chirping waves in the inhomogeneous magnetic field. Despite the rapid change of the parameters during the interaction, we show that the adiabatic invariant is conserved as long as the particles stay trapped in the reference frame moving with the resonance. Assuming the trapped particle distribution as a function of the adiabatic invariant and the water-bag approximation, we derive an analytic form of the nonlinear current as a function of the inhomogeneous parameter that describes the frequency chirping and inhomogeneities in the background magnetic field. The nonlinear current expression is also examined in the Vlasov hybrid simulations and the simulation results show that the nonlinear current can be well described by the adiabatic water bag approximation except for the chirping onset stage and the source region where the adiabatic approximation is invalid.

I. INTRODUCTION

Wave-particle resonant interactions play an important role in a wide range of wave instabilities with frequency chirping in fusion and magnetoshperic plasmas. In the fusion related plasmas, the frequency chirping often appears with the Alfvén wave instabilities [1–4] and energetic-particle-driven geodesic acoustic modes [5]. The wave chirping is usually accompanied by fast ion loss and strong radial transport, which is greatly concerned in the fusion studies. In the planetary magnetosphere, there exists the chorus wave which is a peculiar electromagnetic emission with frequency sweeping in the whistler-mode range of frequencies [6–8]. The chirping behavior similar to the magnetospheric chorus has also been studied recently in the laboratory plasmas [9, 10]. The chorus waves play a critical role in the electron acceleration in the Van Allen radiation belts [11–13] and the pulsating aurora and diffuse auroral precipitation [14–16]. The chorus emission is also related to the studies of the superradiance in free-electron lasers [17, 18].

The physics of the chorus wave in essence are the nonlinear wave-particle interactions [19, 20] between the resonant trapped electrons and the whistler waves [21, 22]. The Hamiltonian treatment of particle nearly resonant with a monochromatic whistler wave in the inhomogeneous magnetic field has been extensively studied [23, 24]. The particle dynamics can be described by a modified pendulum Hamiltonian, where the trapped particles feel both the wave restoring force and the background drag force related to the frequency variation and magnetic field gradient [25, 26].

It is worth noting that the parameters in the Hamiltonian are changing as the frequency varying together with the inhomoegeneous magnetic field. Alike to the pendulum system, if the variation of the parameters are slow compare to the trapped particle bounce motion, then the system is adiabatic and there exists an adiabatic invariant associated with the bounce motion. However, recently studies state that for the chorus frequency chirping problem, the nonlinear chirping timescale τ_{nl} is comparable to the bounce period τ_b. Thus, the interaction is nonadiabatic [27, 28].

Nevertheless, the conventional studies usually manage the particles' dynamics in the laboratory reference frame. In the laboratory reference frame, the wave vector undergoes accelerated rotation due to frequency chirping and the Hamiltonian involves a fast varying phase term in the wave-particle interaction part. However, if we reconsider the interaction on a reference frame that perfectly follows the resonance, i.e., moving in-time with the chirping wave that traps the resonant particle, we would observe no chirping at all. Thus, the fast-varying scale is mitigated and a particle can be regarded as adiabatic as long as it remains trapped. Only the particle near the separatrix region suffers a nonadiabatic motion, as pointed in previous studies [29]. Also, in the early phase of chirping [30], the adiabatic approximation is invalid since the trapped have yet to be established.

In our previous work, we have developed a novel Hamiltonian theory [25]. Harnessing the local resonance frame of reference, we derived the reduced Hamiltonian that describes the interaction of the particle with the slowly varying envelope. With a further restriction to the onset stage of the chirping, we have constructed a corresponding δf Vlasov simulation method and successful obtained the generation of chirping chorus wave. Note that, since the background magnetic field can strongly affect the wave-particle interaction process [31, 32], our simulation is carried with real Earth dipole field configuration. The chirping rate and amplitude are well agreement with satellite observation [33] and PIC simulations with real field parameters [34]. Also, since we choose a static frame that follow the start point of the chirping instead of tracking the chirping with time, the simulation obtains the chirping effect as a slowly varying modulation on the wave envelope.

In this work, we examine the adiabaticity by the test

particle simulation and derive the nonlinear current with adiabatic approximation for the magnetospheric chorus. We introduce a canonical transformation that shifts the static frame to a time-independent reference frame which follows with the real time chirping wave in the Vlasov simulation. For the interaction of chorus waves and energetic electrons, we solve the Hamilton's equations and calculate the adiabatic invariant from the test particle simulations. The energetic electrons move opposite to the motion of the chorus wave packet through several distinct regions with different physical properties. We show that the adiabaticity can be completely different in the different reference frames and in the different regions along the Earth's dipole magnetic fields. In the resonance frame, the adiabatic invariant is preserved in the most of the downstream region where the chorus waves propagate with frequency chirping and grow in amplitudes. As the energetic electrons approach the equator where the chorus waves are triggered with initial small amplitudes, the adiabaticity is no longer valid in the equator and the upstream region due to the particle releasing. From the adiabatic invariant, we further obtain a reduced form of the energetic trapped particle current. We verify the adiabatic approximation from the nonlinear current calculated in the Vlasov simulation and show that the adiabatic regime is valid in the most of downstream region, except in the upstream and equator regions.

The paper is organized as follows. In section II, we review the Hamiltonian theory in the resonance reference frame. In section III, the adiabaticity is examined by the test particle simulation and the nonlinear current is derived with adiabatic approximation. Finally, the summary is presented in section IV.

II. HAMILTONIAN THEORY

In the previous work, the Hamiltonian for the resonant electrons in the frame of reference moving with the local resonance is derived by the canonical transformation [25]. The wave-particle interaction is studied on discrete local spatial cells, and the phase space is described by new canonical coordinates (ξ, Ω), For each cell at a position s_i along the magnetic field, ξ, Ω phase space is decoupled in the original Hamiltonian, and in our hybrid Vlasov simulation [25, 35], the phase flow for the onset of chorus is considered separately with the following Hamiltonian

$$K = \frac{k_l^2\Omega^2}{2} + \mathcal{R}\left(\frac{\omega_b^2}{k_l^2}(e^{-\imath\xi} + \alpha\cdot\xi)\right) \ , \tag{1}$$

where $\mathcal{R}$ denotes taking the real part,

$$\omega_b^2 = \sqrt{2\omega_{ce}(\mathcal{J}+\Pi+\Omega)}k_l^2 a(s_i,t) \tag{2}$$

is the bounce frequency, and

$$\alpha = \frac{k_l}{\omega_b^2}(\mathcal{J} - \frac{\Pi}{2})\frac{d\omega_{ce}}{ds} \ , \tag{3}$$

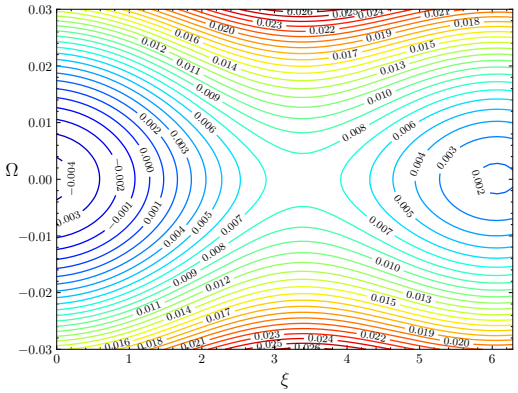

FIG. 1. The contour plot of Hamiltonian in Eq. (1) using fixed $\mathcal{J}, a, \Pi$ parameters.

is the inhomogeneous parameter that describes the frequency chirping and inhomogeneities in the background magnetic field. Other coordinates and variables such as the canonical momentum $\mathcal{J}$, gyro frequency ω_{ce}, and parameter Π are determined from on each local cell [25, 35]. A contour plot of the Hamiltonian is given in Fig. 1

Note that we have fixed the reference frame on the most unstable wave with frequency ω_l and wave number k_l, which corresponds to the onset of the chirping wave. The reference frame we choose is determined from fixed frequency and wave number which does not change with time, thus we refer such reference frame as the static resonance frame hereafter. The simulated wave vector a becomes a complex number with an additional phase $\delta\phi$ due to the static frame can not exactly follow the real time resonance. Therefore we take the real part in the wave-particle interaction term in the above Hamiltonian. The complex wave vector field a can be written as

$$a(s,t) = |a(s,t)|\cdot e^{\imath\delta\phi(s,t)} \ , \tag{4}$$

where $\delta\phi$ can be regarded as a modulation on the wave envelope, as shown in Fig. 2.

The varying phase $\delta\phi(s,t)$ indicates the acceleration of trapped particles along Ω momentum dimension in phase space. Combining the calculated wave fields in the Vlasov simulation [25], we solve the equations of motion using the Hamiltonian in Eq. (1) and show the particle phase space trajectories in Fig. 3(a). In the static resonance frame, trapped particles do not have a closed phase space trajectory and their angle variable ξ is shifting and matching with the wave phase $\delta\phi$ along its trajectory, as illustrated in Fig. 3(b). This is in accordance with the phase locking condition [26]. Their momenta, as shown in Fig. 3(c), are also accelerating upwards along Ω dimension due to the rising tone frequency chirping.

Since the wave phase $\delta\phi$ can be calculated from the Vlasov simulation [25], we can construct a canonical transformation to shift the static resonance frame back to the real-time resonance frame of reference. To do so, the new angle variable and momentum take the following

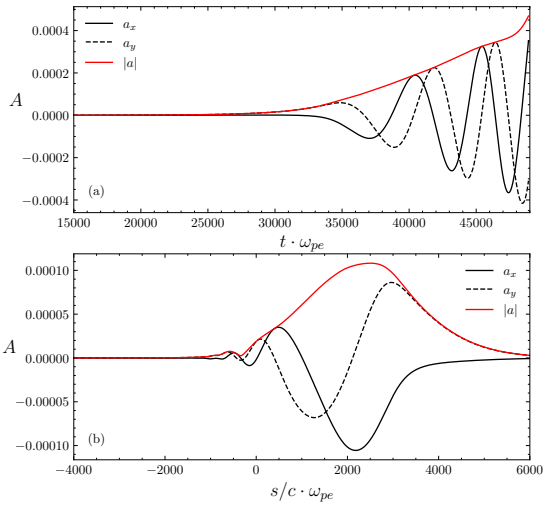

FIG. 2. (a) Time evolution and (b) spatial distribution of the orthogonal components of vector potential, a_x and a_y, and the amplitude $|a|$ in the simulation.

forms [36],

$$\begin{aligned} Q &= \xi - \delta\phi(s(t), t) \ , \\ P &= \Omega - f(t) \ , \end{aligned} \tag{5}$$

where $f(t)$ is a time dependent function to be determined. The above transformation corresponds to a type-2 generating function

$$F_2(\xi, P, t) = (\xi - \delta\phi) \cdot P + \xi \cdot f(t) \tag{6}$$

and the corresponding new Hamiltonian K' is

$$\begin{aligned} K' &= K + \frac{\partial F_2}{\partial t} \\ &= \frac{k_l^2}{2}(P + f(t))^2 + \sqrt{2\omega_{ce}(\mathcal{J} + P + f(t) + \Pi)} \cdot |a| \cos(Q) \\ &+ ((\frac{1}{k_l}(\mathcal{J} - \frac{\Pi}{2})\frac{d\omega_{ce}}{ds}) + \frac{df(t)}{dt}) \cdot (Q + \delta\phi) - \frac{d\delta\phi}{dt} P \ . \end{aligned} \tag{7}$$

In addition, the first order term with respect to P should be eliminated in the above Hamiltonian, which determines $f(t)$ as

$$f(t) = -\frac{1}{k_l^2}\frac{d\delta\phi}{dt} \quad = \frac{\delta\omega - v_r \delta k}{k_l^2} \ . \tag{8}$$

Note that the exact time derivative is evaluated along the particle trajectory, $d/dt = \partial/\partial t + v_r \partial/\partial s$ with $\delta\omega \equiv \partial\delta\phi/\partial t$ and $\delta k \equiv -\partial\delta\phi/\partial s$. We can examine that $f(t)$ is the first order variation of $\Omega(\omega, k)$ due to the chirping frequency $\delta\omega$, and the variation of wave number δk. The expression also agrees with the change of Ω in the test particle results shown in Fig. 3(c). For the derivative of $f(t)$, we only keep the term up to the first order, which gives

$$\frac{df(t)}{dt} \simeq \frac{1}{k_l^2}(\frac{\partial\delta\omega}{\partial t} + 2v_r\frac{\partial\delta\omega}{\partial s} + \frac{3}{2}v_r\frac{\delta k}{k_l}\frac{d\omega_{ce}}{ds}). \tag{9}$$

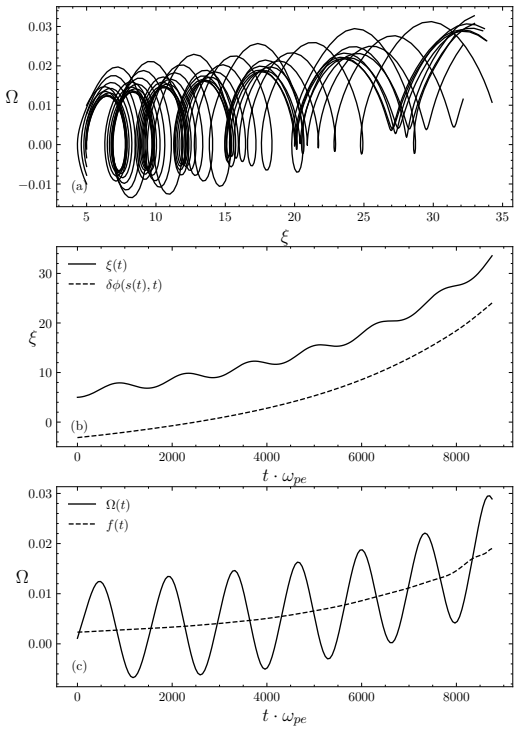

FIG. 3. (a) Phase space trajectories of test particles with initial angle $\xi = 5$ sampled in $\Omega \in [-0.01, 0.01]$, (b) typical variation of angle coordinate ξ of a test particle and the cooresponding wave phase $\delta\phi$ along its trajectory. (c) the corresponding variation of particle momentum Ω with time. The dashed line denotes Eq. (8).

Finally, the new Hamiltonian takes the following form

$$K' = \frac{k_l^2 P^2}{2} + \frac{\omega_b^2}{k_l^2}(\cos Q + \alpha \cdot Q) \ , \tag{10}$$

where

$$\omega_b^2 = \sqrt{2\omega_{ce}(\mathcal{J} + P + f(t) + \Pi)} k_l^2 |a| \tag{11}$$

and we have a new α

$$\begin{aligned} \frac{\omega_b^2}{k_l^2}\alpha &= \frac{1}{k_l}\left(\mathcal{J} - \frac{\Pi}{2}\right)\frac{d\omega_{ce}}{ds} \\ &+ \frac{1}{k_l^2}\left(\frac{\partial\delta\omega}{\partial t} + 2v_r\frac{\partial\delta\omega}{\partial s} + \frac{3}{2}v_r\frac{\delta k}{k_l}\frac{d\omega_{ce}}{ds}\right) \ . \end{aligned} \tag{12}$$

The additional terms compared to Eq. (3) first order correction related to frequency chirping and wave number variation.

Using the new Hamiltonian, we are able to consider the particle dynamics in real-time resonance frame of reference. To show the differences, we choose a test particle initially at the resonance center and calculate its phase space trajectories in the different reference frames in Fig. 4. In the static resonance frame, the particle suffers a rapid change in Ω for each bounce in accordance with Fig. 3(a). In contrast, there exists only a slight change

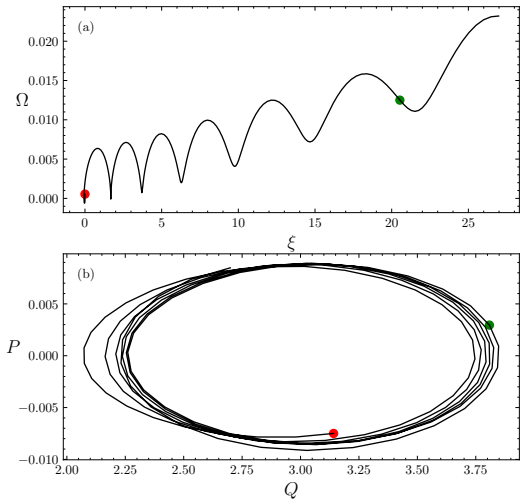

FIG. 4. Phase space trajectory of a test particle from $s = 700$ at $t = 750$ to $s = 520$ at $t = 930$ (a) in the static resonance frame and (b) in the real-time resonance frame. The red dot denotes the start point, and the green dot denotes $t = 910$.

when we track the particle in the real-time resonance frame, which demonstrates the effectiveness of the canonical transformation.

III. ADIABATIC APPROXIMATION

For the resonant electrons trapped by the slowly varying wave envelope and circling around in the phase space, the adiabatic invariant is defined as

$$\mathcal{I} = \frac{1}{2\pi} \oint \Omega(H, \xi, t) \mathrm{d}\xi \ , \tag{13}$$

where Ω is an implicit function of the Hamiltonian H. Using the Hamiltonian (1) and (10), we can numerically calculate the adiabatic invariant $\mathcal{I}$ in the static and moving resonance frames, respectively.

For each temporospatial location, with fixed background and wave parameters, we are able to complete a closed trajectory if particle is trapped in the wave field. The area of the enclosed loop is actually the phase space integral $\mathcal{I}$. In the static frame, it is clear that the area changes significantly, as shown in Fig. 5(a). In the moving frame, the area changes much smaller, suggesting the validity of the particle adiabatic motion. To quantitatively show the adiabaticity, we numerically calculate the area of the phase loop and show its time variation and the relative error of the adiabatic invariant $\mathcal{I}(t)$ in Fig. 6. Unlike the static frame, the variation of $\mathcal{I}$ is less than 2% in the reference frame following with the resonance, as seen in Fig. 6(d). This shows the conservation of the adiabatic invariant $\mathcal{I}$ and the validity of the adiabaticity. The variation becomes large until the particle approaches to the equator, where the wave amplitude is small and the particle can be released from the wave potential well.

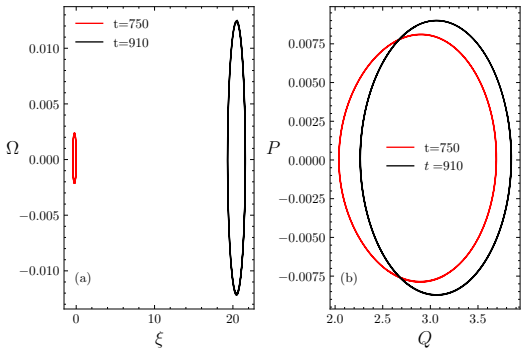

FIG. 5. Enclosed phase space loop of a particle at different times.

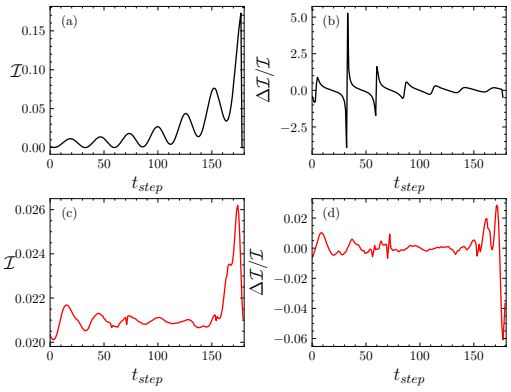

FIG. 6. Time variation and relative change of $\mathcal{I}$ of a given particle in the static (the black lines) and real-time resonance frames (the red lines).

The releasing of trapped particle, which is reported in the particle in cell (PIC) simulation [26], could be a potential reason for the violation of the adiabatic motion.

With the adiabatic approximation, we can greatly reduce the description of the trapped particle distribution and the energetic particle current. The nonlinear energetic particle current j_p is obtained from the velocity integral of the perturbed distribution function [25]

$$j_p(s_i, t) = -\frac{1}{4\pi} \frac{\omega_{h0}^2 k_i}{e} \iiint \sqrt{2 m_e \omega_{ce}(s)(\mathcal{J} + \Omega + \Pi_i)} \times f(\xi, \Omega, \mathcal{J}; s_i(t), t) e^{\imath\xi} \mathrm{d}\xi \mathrm{d}\Omega \mathrm{d}\mathcal{J} \ . \tag{14}$$

At the nonlinear stage, the distribution function of the trapped electrons forms a hole in phase space. Since the equilibrium distribution does not contribute to the current, the nonlinear current is directly determined by the deviation from the unperturbed distribution, i.e., the depth of the hole, Δf. The depth of the hole can be written as the function of the adiabatic invariant, i.e., $\Delta f(s_i, \mathcal{J}, \mathcal{I}, \xi, t)$. Now we replace f by Δf in the cur-

rent integral in Eq. (14) and write the integral as

$$j_p(s_i,t) \approx -\int \mathrm{d}\mathcal{J}\sqrt{2\omega_{ce}(\mathcal{J}+\Pi_i(t))} \times \int_0^{\mathcal{I}_{\rm spx}} \mathrm{d}\mathcal{I} \oint \mathrm{d}\psi \Delta f(s_i,\mathcal{J},\mathcal{I},\xi,t)e^{\imath\xi} \ . \tag{15}$$

Note that Ω in the square root has been neglected since $\Omega \simeq 0$. The differential area element $\mathrm{d}\xi\mathrm{d}\Omega$ is changed to $\mathrm{d}\mathcal{I}\mathrm{d}\psi$, where ψ is the angle variable of $\mathcal{I}$. From the Jacobi of the differential element, the integral over ψ is

$$\oint f\mathrm{d}\psi = \oint f\frac{\mathrm{d}\Omega}{\mathrm{d}\mathcal{I}}\mathrm{d}\xi = \frac{\partial H}{\partial \mathcal{I}}\oint f\frac{\mathrm{d}\Omega}{\mathrm{d}H}\mathrm{d}\xi = \dot{\psi}\oint \frac{f}{\Omega}\mathrm{d}\xi = 2\pi\langle f\rangle, \tag{16}$$

where $\langle\cdots\rangle$ denotes the bounce average following the definition in Ref. [36]. Thus the current integral becomes

$$j_p(s_i,t) \approx -2\pi\int \mathrm{d}\mathcal{J}\sqrt{2\omega_{ce}(\mathcal{J}+\Pi_i(t))} \times \int_0^{\mathcal{I}_{\rm spx}} \mathrm{d}\mathcal{I}\langle\Delta f(s_i,\mathcal{J},\mathcal{I},\xi,t)e^{\imath\xi}\rangle \ . \tag{17}$$

Note that Δf can be expanded in powers of ϵ, a small parameter describing the change of parameters during the bounce motion and the bounce averages in Eq. (17) are [36]

$$\begin{aligned}\langle\Delta f\sin\xi\rangle &\simeq \alpha\Delta f_0 \ ,\\ \langle\Delta f\cos\xi\rangle &\simeq \Delta f_0\langle\cos\xi\rangle \ .\end{aligned} \tag{18}$$

We further assume that Δf_0 is independent of $\mathcal{I}$, which implies that the depth of the hole is flat within the enclosed hole area, i.e., the water bag approximation [21, 37]. Therefore, the integral over $\mathcal{I}$ only depend on the $\mathcal{I}_{\rm spx}$ which is the adiabatic invariant on the separatrix. According to Eq. (13), we have

$$\int_0^{\mathcal{I}_{\rm spx}}\mathrm{d}\mathcal{I} = \mathcal{I}_{\rm spx} \equiv \frac{1}{2\pi}\oint_{\rm spx}\Omega(\xi)\mathrm{d}\xi \ , \tag{19}$$

where the boundary of the trapped particle phase space hole can be analytically given as

$$\Omega(\xi) = \pm\frac{\omega_b}{k^2}\sqrt{2(e_{\rm spx}-\cos\xi-\alpha\xi)} \ , \tag{20}$$

and $e_{\rm spx}$ denotes the Hamiltonian on the separatrix. Then the current integral becomes

$$j_p(s_i,t) \approx \frac{\sqrt{2}\omega_b}{k^2}\left(m_{\rm spx}+\imath\ n_{\rm spx}\right) \times \int \mathrm{d}\mathcal{J}\sqrt{\omega_{ce}(\mathcal{J}+\Pi_i(t))}\Delta f(\mathcal{J},s_i,t) \ , \tag{21}$$

where

$$\begin{aligned} m_{\rm spx}(\alpha) &= \oint_{\rm spx}\mathrm{d}\xi\cos\xi\sqrt{e_{\rm spx}-\cos\xi-\alpha\xi},\\ n_{\rm spx}(\alpha) &= \alpha\oint_{\rm spx}\mathrm{d}\xi\sqrt{e_{\rm spx}-\cos\xi-\alpha\xi}. \end{aligned} \tag{22}$$

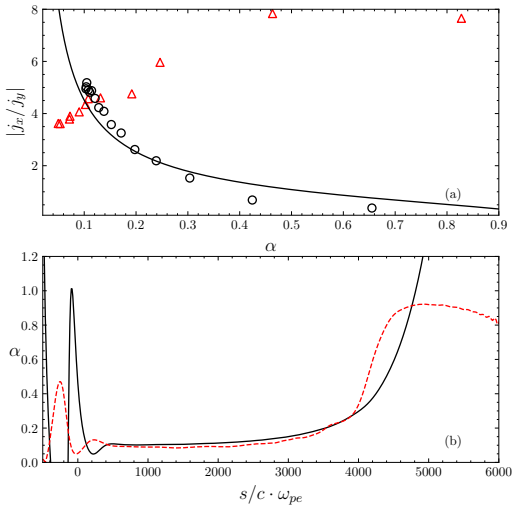

FIG. 7. (a) Current ratio versus the inhomogeneous parameter α. The scattered points are obtained at difference spatial locations from the simulation, the triangles are obtained from near equator region while circus are obtained from the downstream region. The solid curve is the results from adiabatic approximation Eq. (23). (b) Snapshot of the parameter α at $t = 850$ obtained from the definition in Eq. (12) (black solid line) and from adiabatic relation (red dashed line).

The temporospatial evolution of the nonlinear current only depends on the integral over the slowly varying scale $\mathcal{J}$, and an inhomogeneity parameter α, defined in Eq. (12). The $\mathcal{J}$ integral can be calculated further with the adiabatic motion of the trapped particle along the magnetic field line [38], while the integrals $m_{\rm spx}$ and $n_{\rm spx}$ can be numerical integrated from Eq. (22). Note that, our Vlasov simulation is performed with Hamiltonain Eq. (1), thus the phase of the current j_p in the Vlaov simulation also differs $\delta\phi$ with the current relation in Eq. (21). To compared and verify our adiabatic theory, we should also translate this addition phase, i.e., $j_p' = j_p\cdot e^{-\imath\delta\phi}$, where j_p is the current from Vlasov equation. Now we can show the validity of the adiabatic approximation by examining the ratio of the imaginary and real component of j_p',

$$\begin{aligned}\frac{j_x}{j_y} &= \frac{\mathrm{real}(j_p')}{\mathrm{imag}(j_p')} = \frac{m_{\rm spx}}{n_{\rm spx}}\\ &= \frac{\oint_{\rm spx}\mathrm{d}\xi\cos\xi\sqrt{e_{\rm spx}-\cos\xi-\alpha\xi}}{\alpha\oint_{\rm spx}\mathrm{d}\xi\sqrt{e_{\rm spx}-\cos\xi-\alpha\xi}}.\end{aligned} \tag{23}$$

The current ratio as function of α is calculated from Eq. (21) and compared with the nonlinear current in the Vlasov simulation [25, 35]. The corresponding α is obtained from its definition using the simulation data. Figure 7 shows that the simulation results in a wide spatial range from the magnetic equator to the high latitude region (black triangles) well agree with the adiabatic approximation. While near the equator region (red circles),

the adiabatic approximation is no longer valid. Similar conclusion can be drawn from the spatial distribution of α calculated from definition in Eq. (12) and the adiabatic current relation, as shown in Fig. 7(b). The evolution of α indicates a rapid variation of the phase space near the equator, which is related to the generation of the nonlinear chorus wave. The results of nonadiabtic regime also agree with the previous PIC simulations [27, 28].

IV. CONCLUSION

In summary, we have explored the dynamics of resonant electrons and the evolution of whistler-mode chorus waves by test particle simulations. We show that the adiabatic description is valid if one tracks the dynamics in the frame of reference moving the local resonance. We have derived an analytic current expression and discussed the adiabatic regime in the global domain by showing the wave chirping behavior with respect to the inhomogeneity parameter α. The adiabatic approximation and the reduced current expression reveal the underlying physics for the wave chirping.

ACKNOWLEDGMENTS

The work was inspired by H.L.Berk during Ge Wang worked with him at the University of Texas. As Herb's former Ph.D. student and long-time collaborator, Ge witnessed Herb's kindness, diligence, and persistence. Thank you, Herb. This work was supported by the National Natural Science Foundation of China under Grant No. 12275013. The simulations were carried out at National Supercomputer Center in Tianjin and performed on Tianhe new generation supercomputer.

[1] L. Chen and F. Zonca, Physics of Alfvén waves and energetic particles in burning plasmas, Rev. Mod. Phys. **88**, 72 (2016).
[2] G. Wang, H. Berk, B. Breizman, and L.-J. Zheng, Frequency chirping in the Alfvén continuum, Nuclear Fusion **58**, 082014 (2018).
[3] G. Wang and H. Berk, Simulation and theory of spontaneous TAE frequency sweeping, Nucl. Fusion **52**, 094003 (2012).
[4] G. Wang and H. Berk, Model for spontaneous frequency sweeping of an Alfvén wave in a toroidal plasma, Communications in Nonlinear Science and Numerical Simulation **17**, 2179 (2012).
[5] H. Wang, Y. Todo, and C. C. Kim, Hole-Clump Pair Creation in the Evolution of Energetic-Particle-Driven Geodesic Acoustic Modes, Physical Review Letters **110**, 155006 (2013).
[6] R. Helliwell, *Whistlers and Related Ionospheric Phenomena* (Stanford University Press, 1965).
[7] W. Burtis and R. Helliwell, Magnetospheric chorus: Occurrence patterns and normalized frequency, Planetary and Space Science **24**, 1007 (1976).
[8] B. T. Tsurutani and E. J. Smith, Postmidnight chorus: A substorm phenomenon, Journal of Geophysical Research (1896-1977) **79**, 118 (1974).
[9] B. Van Compernolle, X. An, J. Bortnik, R. M. Thorne, P. Pribyl, and W. Gekelman, Excitation of Chirping Whistler Waves in a Laboratory Plasma, Physical Review Letters **114**, 245002 (2015).
[10] H. Saitoh, M. Nishiura, N. Kenmochi, and Z. Yoshida, Experimental study on chorus emission in an artificial magnetosphere, Nat Commun **15**, 861 (2024).
[11] R. B. Horne, R. M. Thorne, Y. Y. Shprits, N. P. Meredith, S. A. Glauert, A. J. Smith, S. G. Kanekal, D. N. Baker, M. J. Engebretson, J. L. Posch, M. Spasojevic, U. S. Inan, J. S. Pickett, and P. M. E. Decreau, Wave acceleration of electrons in the Van Allen radiation belts, Nature **437**, 227 (2005).
[12] R. M. Thorne, W. Li, B. Ni, Q. Ma, J. Bortnik, L. Chen, D. N. Baker, H. E. Spence, G. D. Reeves, M. G. Henderson, C. A. Kletzing, W. S. Kurth, G. B. Hospodarsky, J. B. Blake, J. F. Fennell, S. G. Claudepierre, and S. G. Kanekal, Rapid local acceleration of relativistic radiation-belt electrons by magnetospheric chorus, Nature **504**, 411 (2013).
[13] G. D. Reeves, H. E. Spence, M. G. Henderson, S. K. Morley, R. H. W. Friedel, H. O. Funsten, D. N. Baker, S. G. Kanekal, J. B. Blake, J. F. Fennell, S. G. Claudepierre, R. M. Thorne, D. L. Turner, C. A. Kletzing, W. S. Kurth, B. A. Larsen, and J. T. Niehof, Electron Acceleration in the Heart of the Van Allen Radiation Belts, Science **341**, 991 (2013).
[14] Y. Nishimura, J. Bortnik, W. Li, R. M. Thorne, L. R. Lyons, V. Angelopoulos, S. B. Mende, J. W. Bonnell, O. Le Contel, C. Cully, R. Ergun, and U. Auster, Identifying the Driver of Pulsating Aurora, Science **330**, 81 (2010).
[15] S. Kasahara, Y. Miyoshi, S. Yokota, T. Mitani, Y. Kasahara, S. Matsuda, A. Kumamoto, A. Matsuoka, Y. Kazama, H. U. Frey, V. Angelopoulos, S. Kurita, K. Keika, K. Seki, and I. Shinohara, Pulsating aurora from electron scattering by chorus waves, Nature **554**, 337 (2018).
[16] R. M. Thorne, B. Ni, X. Tao, R. B. Horne, and N. P. Meredith, Scattering by chorus waves as the dominant cause of diffuse auroral precipitation, Nature **467**, 943 (2010).
[17] F. Zonca, X. Tao, and L. Chen, Nonlinear dynamics and phase space transport by chorus emission, Reviews of Modern Plasma Physics **5**, 8 (2021).
[18] A. R. Soto-Chavez, A. Bhattacharjee, and C. S. Ng, Chorus wave amplification: A free electron laser in the Earth's magnetosphere, Physics of Plasmas **19**, 010701 (2012).
[19] T. M. O'Neil, Nonlinear Interaction of a Small Cold Beam and a Plasma, Physics of Fluids **14**, 1204 (1971).
[20] T. M. O'Neil, Nonlinear Interaction of a Small Cold Beam and a Plasma. Part II, Physics of Fluids **15**, 1514 (1972).

[21] Y. Omura, Y. Katoh, and D. Summers, Theory and simulation of the generation of whistler-mode chorus, Journal of Geophysical Research: Space Physics **113**, 10.1029/2007JA012622 (2008).

[22] X. An, J. Li, J. Bortnik, V. Decyk, C. Kletzing, and G. Hospodarsky, Unified View of Nonlinear Wave Structures Associated with Whistler-Mode Chorus, Physical Review Letters **122**, 045101 (2019).

[23] J. M. Albert, Cyclotron resonance in an inhomogeneous magnetic field, Physics of Fluids B: Plasma Physics , 8 (1993).

[24] J. M. Albert, A. V. Artemyev, W. Li, L. Gan, and Q. Ma, Models of Resonant Wave-Particle Interactions, J. Geophys. Res. Space Phys. **126**, e2021JA029216 (2021).

[25] J. Zheng, G. Wang, and B. Li, A Hamiltonian theory for nonlinear resonant wave–particle interaction in weakly inhomogeneous magnetic field, Phys. Plasmas **31**, 042104 (2024).

[26] X. Tao, F. Zonca, and L. Chen, A "Trap-Release-Amplify" Model of Chorus Waves, Journal of Geophysical Research: Space Physics **126**, e2021JA029585 (2021).

[27] X. Tao, F. Zonca, and L. Chen, Investigations of the electron phase space dynamics in triggered whistler wave emissions using low noise δf method, Plasma Physics and Controlled Fusion **59**, 094001 (2017).

[28] X. Tao, F. Zonca, and L. Chen, Identify the nonlinear wave-particle interaction regime in rising tone chorus generation, Geophysical Research Letters **44**, 3441 (2017).

[29] J. R. Cary and R. T. Skodje, Phase change between separatrix crossings, Phys. Nonlinear Phenom. **36**, 287 (1989).

[30] A. Bierwage, R. B. White, and V. N. Duarte, On the Effect of Beating during Nonlinear Frequency Chirping, Plasma and Fusion Research **16**, 1403087 (2021).

[31] Z. Wu, H. Huang, Y. Wu, X. Tao, Y. Katoh, and X. Wang, Connection Between Chorus Wave Amplitude and Background Magnetic Field Inhomogeneity: A Parametric Study, Geophysical Research Letters **50**, e2023GL106397 (2023).

[32] Y. Wu, X. Tao, F. Zonca, L. Chen, and S. Wang, Controlling the Chirping of Chorus Waves via Magnetic Field Inhomogeneity, Geophysical Research Letters **47**, 10.1029/2020GL087791 (2020).

[33] C. M. Cully, V. Angelopoulos, U. Auster, J. Bonnell, and O. Le Contel, Observational evidence of the generation mechanism for rising-tone chorus: CHORUS CHIRP RATES, Geophysical Research Letters **38**, n/a (2011).

[34] Y. Katoh and Y. Omura, Electron hybrid code simulation of whistler-mode chorus generation with real parameters in the Earth's inner magnetosphere, Earth, Planets and Space **68**, 192 (2016).

[35] J. Zheng, G. Wang, and B. Li, A hybrid eulerian-lagrangian vlasov method for nonlinear wave-particle interaction in weakly inhomogeneous magnetic field, submitted to Computer Physics Communications (2023).

[36] H. L. Berk, B. N. Breizman, J. Candy, M. Pekker, and N. V. Petviashvili, Spontaneous hole–clump pair creation, Physics of Plasmas **6**, 3102 (1999).

[37] H. Hezaveh, Z. S. Qu, M. J. Hole, and R. L. Dewar, Theoretical description of chirping waves using phase-space waterbags, Plasma Physics and Controlled Fusion **63**, 065008 (2021).

[38] D. Summers, Y. Omura, Y. Miyashita, and D.-H. Lee, Nonlinear spatiotemporal evolution of whistler mode chorus waves in Earth's inner magnetosphere: SPATIOTEMPORAL EVOLUTION OF CHORUS, J. Geophys. Res. **117**, n/a (2012).